December 17, 2004

Station Configuration Studies Writeup

Emil Polisensky

ABSTRACT

First draft writeup of the LWA/LWDA station configuration studies I've been working on.

1. Introduction

I've been investigating various designs for the placement of elements within a station for the LWDA and LWA. A station consists of an array of 256 elements where each element is 2 crossed dipole antennas. I assume the elements are placed on flat ground and I define a rectangular coordinate system (x, y, z) such that x point East, y points North, and z points to the zenith with distances measured in meters. Directions in the sky are given by rectangular coordinates (l, m, n) of a point on a celestial sphere of unit radius. Since $l^2 + m^2 + n^2 = 1$, directions in the sky can be given by just (l, m).

2. Equations

The field pattern of an array is a complex function describing the amplitude and phase of the voltage at an element as a function of the direction of arrival of waves from a distant source of constant strength but variable direction. The phase term is relative to that of an element at the origin of the coordinate system. The field pattern of a planar array is given by:

$$F(l,m) = const \times F_e(l,m) \times \iint_{-\infty}^{+\infty} g(x,y) \times e^{-i\frac{2\pi}{\lambda}(xl+ym)}\, dx\, dy$$

where $F_e(l, m)$ is the field pattern of an individual element and $g(x, y)$ is called the grading function. The grading function assigns a number between 0 and 1 (a weight) to each element and is zero everywhere else. The constant normalizes the field pattern to the maximum. Define $f(l, m)$ to be the fourier transform of the grading:

$$f(l,m) = \iint_{-\infty}^{+\infty} g(x,y) \times e^{-i\frac{2\pi}{\lambda}(xl+ym)}\, dx\, dy$$

The field pattern equation then becomes:

$$F(l,m) = const \times F_e(l,m) \times f(l,m)$$

The power pattern is the square of the field pattern modulus:

$$P(l,m) = |F(l,m)|^2$$

My studies have been concerned with the positions of elements on the ground, not on the elements themselves, so I have taken the element field pattern to be 1 over all space (isotropic dipoles). The field pattern then becomes:

$$F(l,m) = const \times f(l,m)$$

The field and power patterns then depend on the fourier transform of the grading function only.

The above equations are valid for an array pointed at the zenith ($l = 0, m = 0$). Steering the beam to point in a new direction, (l_{ref}, m_{ref}), is equivalent to changing the grading from $g(x,y)$ to $g(x,y) \times e^{i\frac{2\pi}{\lambda}\left(xl_{ref}+ym_{ref}\right)}$ The fourier transform becomes:

$$f(l,m) = \iint_{-\infty}^{+\infty} g(x,y) \times e^{-i\frac{2\pi}{\lambda}\left(x\left(l-l_{ref}\right)+y\left(m-m_{ref}\right)\right)}\, dx\, dy$$

A real array has a finite number of discrete elements (N) and the integrals can be replaced with a finite sum:

$$f(l,m) = \sum_{k=1}^{N} g_k \times e^{-i\frac{2\pi}{\lambda}\left(x_k\left(l-l_{ref}\right)+y_k\left(m-m_{ref}\right)\right)}$$

Using Euler's identity this can be written:

$$f(l,m) = \Re(f) - i\Im(f) = Ve^{-i\phi}$$

where:

$$\Re(f) = \sum_{k=1}^{N} g_k \times \cos\left(\frac{2\pi}{\lambda}\left[x_k\left(l-l_{ref}\right)+y_k\left(m-m_{ref}\right)\right]\right)$$

$$\Im(f) = \sum_{k=1}^{N} g_k \times \sin\left(\frac{2\pi}{\lambda}\left[x_k\left(l-l_{ref}\right)+y_k\left(m-m_{ref}\right)\right]\right)$$

$$V = \sqrt{\left(\Re(f)\right)^2 + \left(\Im(f)\right)^2}$$

The normalizing constant in the field pattern equation is just:

$$const = \left(\sum_{k=1}^{N} g_k \right)^{-1}$$

and the power pattern is thus:

$$P(l,m) = (const \times V)^2$$

3. Metrics

Beam Size

The size of the beam is defined as the FWHM of the power pattern, the angular extent of the points where the power falls to half its maximum value (-3 dB points). Since the beam may not be circularly symmetric the beam size metric is defined as:

$$Beam\ Size = (B_{major} \times B_{minor})^{1/2}$$

where B_{major} and B_{minor} are the largest and smallest angular extents of the beam. The beam size metric indicates how large the beam is while taking into account any distortion from circular symmetry.

Beam Efficiency

The beam efficiency metric is defined as the ratio of the power pattern integrated over the solid angle of the main beam to the integral of the power pattern over the whole sky:

$$Beam\ Efficiency = \frac{\int_{MainBeam} P(l,m)\, d\Omega}{\int_{4\pi} P(l,m)\, d\Omega}$$

The beam efficiency metric gives an indication of the amount of power in the main beam versus the amount spread around in sidelobes.

I let $P(l,m) = 0$ below the horizon.

Aperture Efficiency

The aperture efficiency metric is defined as the ratio of the effective area to the physical area of the station.

$$Aperture\ Efficiency = \frac{A_{effective}}{A_{physical}}$$

The effective area is defined as:

$$A(l, m) = A_{max} \times P(l, m)$$

The effective area depends on frequency and on direction in the sky. To investigate how the aperture efficiency changes with frequency I decided to hold the sky direction constant as the direction of maximum response. The effective area is a maximum in the direction of maximum response and is given by:

$$A_{max} = \frac{\lambda^2}{\int_{4\pi} P(l, m)\, d\Omega}$$

For the physical area of the station I just used $\pi \times r^2$. And I again let $P(l, m) = 0$ below the horizon.

Cable length

This metric is important for cost analysis. The signal from each element will need to be brought to an electronics box to be sent to a computer. The location of the box in a station has not been specified, so I calculate the cable length by simply adding the distances of each element from the center of the station.

4. LWDA1 Station Layouts

The original idea for the 1st prototype station (LWDA1) was for the station to have the same field of view as a VLA dish at 74 MHz but with 10 times the sensitivity. Now there is the idea of making the LWDA1 look like a full LWA station. A decision regarding these 2 ideas has not been reached. In this section I consider the original LWDA1 designs, optimized for 74 MHz. All stations have 256 elements.

I started with a simple square grid design with 2m separation between rows and columns. See Figure 1. The grid has a diagonal diameter of 42.4m.

I also generated layouts with elements placed randomly within a 50m diameter circle and a certain minimum spearation between elements. Figure 2 is a random station with a minimum element separation of 2m. Figure 3 has a minimum separation of 1.8m.

Figure 4 is a design made by Pat Crane. This layout starts with the elements placed on a grid, then radially stretches the outer elements. The amount of stretching depends on distance from the center:

$$d_{new} = \frac{d_{old}^2}{d_{min}}$$

In Figure 4 the inner elements are on a 2m grid while all elements beyond 12.5m (d_{min}) from the center have been stretched radially. Pat's design has 120 elements on the grid and 136 elements in the outer, stretched, parts of the station.

I made some variants on Pat's design keeping the central grid but placing the outer elements on spirals. Figures 5, 6, 7, and 8 show designs with 1, 2, 3, and 4 arm spirals respectively.

I made some fractal layouts following the design of Jaap Bregman (Bregman 1999; Bregman 2000; Bregman et al. 2000). Jaap's stations are composed of 4 concentric rings with exponentially increasing radius. Each ring has 8 clusters and each cluster has 8 elements. Jaap calls this a "two level fractal" configuration. Each ring is optimized for a particular frequency such that each cluster in a ring is a square with side = λ. Two elements are placed on a side, half a wavelength apart and a quarter wavelength from the end of the side.

Figure 9 shows the fractal layout I made following Jaap's design. The rings have clusters with sides of $\lambda = 3.75, 5.0, 7.5, 15.0$m corresponding to frequencies of 20, 40, 60, and 80 MHz respectively. The diameter of the fractal station is 113m, much greater than the other layouts. I designed a smaller fractal station by keeping the same cluster sizes but reducing the distance between rings. Instead of exponetially increasing ring radius, I made the distance as close as possible by letting the closest elements between rings be 3.75m apart. This "compact" fractal design is shown in Figure 10. The diameter of the compact fractal is 97m. An even tighter fractal design would be possible by placing the smallest, inner ring inside of the largest, outer ring and then moving all rings closer to the center. Jaap even suggests doing this (Bregman 2000; Bregman et al. 2000), but I haven't generated such a layout yet. Even so, I don't think the fractal design can fit in a 50m diameter. The fractal designs are included in comparison with the 50m diameter layouts but they will also be included in LWA station design studies.

4.1. Metrics

Plots of the metrics for the LWDA1 stations are given in this section. The same color/symbol key is used throughout the figures and is given below:

• = grid	• = random 2m	□ = random 1.8m
□ = fractal	• = compact fractal	• = Pat's
• = 1 arm spiral	□ = 2 arm spiral	○ = 3 arm spiral
⋆ = 4 arm spiral		

Beam Size

The beam size metric for the LWDA1 stations is shown in Figure 11. It can be seen the beam size depends largely on the physical extent of the station. The grid station is the smallest physically and it has the largest beam at all frequencies. The fractal stations are the largest and have the smallest beams. This makes sense when considering the size of the station in terms of wavelengths. At low frequencies/long wavelengths the size of the station is smaller than at high frequencies/short wavelengths. An infinitely small station would be a point and radiate isotropically. An infinite plane station would radiate in only one direction.

The placement of the elements in a station also effects the beam size. Compare the random stations which are uniformly spread around the full station area with Pat's and the spirals whose elements are centrally condensed. The centrally condensed stations produce larger beams than stations whose elements are more spread out.

Beam Efficiency

The beam efficiency plot is given in Figure 12. Two striking features of this plot are the remarkable flatness of the metric for the grid station and the dominance of the 4 arm spiral over Pat's and the other spirals above 60 MHz. Both features are related to the sensitivity of the metric to sidelobe levels.

Figure 13 shows E-W slices through the beam pattern of the grid layout for several frequencies. The narrowing of the main beam with increasing frequency is readily apparent. It will also be noticed, as frequency increases and the main beam narrows, the sidelobes narrow and move closer to the main beam with new sidelobes appearing on the horizon. The new sidelobes have a lower amplitude than the sidelobes that used to be on the horizon. In terms of the metric the narrowing reduces the solid angle of the main beam and reduces the integral in the numerator. This reduces the all sky integral also but the all sky integral will be further reduced because the new sidelobes have lower amplitudes. I think these effects are decreasing the numerator and denominator by roughly the same amount as the frequency increases and results in the metric staying fairly constant.

Further evidence of the effect of sidelobes on the metric is shown in Figure 14. The metric for grid stations with various separtions between elements is plotted. For each station grating lobes appear on the horizon at a frequency with wavelength equal to the element separation. For the 4m grid grating lobes appear at 75 MHz. The lobes drop the metric dramatically (at higher frequencies, the grating lobes move to higher elevations and the metric begins to increase). Even before the lobes appear the metric is decreasing. This is due to increasing

sidelobe levels as Figure 15 shows. Before the grating lobes appear, the sidelobes on the horizon are larger than the lobes they replace. This increases the all sky integral and causes the metric to decrease.

Sidelobes also explain why the 4 arm spiral has a higher metric than Pat's and the other spirals above 60 MHz. Figures 16 and 17 show E-W power patterns for the 4 arm spiral and Pat's design. At 60 MHz a significant lobe (> -30 dB) has already appeared for Pat's design and the metric has begun to decrease (the other spirals are similar). For the 4 arm spiral a significant lobe doesn't appear until about 70 MHz, at which point the metric begins to decrease.

The fractal stations have a much lower beam efficiency than the other stations, but this could be due to the larger size/smaller main beam of the fractals. The fractals will be examined in comparison to larger stations in the next section.

Aperture Efficiency

Aperture efficiency is plotted in Figure 18. Qualitatively the plot for each station has a similar shape to its beam efficiency plot. This is not suprising since both metrics contain an all sky integral of the power pattern in the denominator. Quantitatively the metrics are different. For example, the random stations have very high aperture efficiencies at the low frequencies. One of the random stations even has a metric > 1 at 20 MHz, but I think this is just an artifact of the numerical integration.

Cable Lengths

Table 1 gives cable lengths for these layouts. Layouts are sorted from smallest to largest length.

5. LWA Stations

An LWA station should have a diameter larger than 50m to be more sensitive at lower frequencies. The simplest thing to do is to take the 50m diameter LWDA1 stations and scale them up to larger size. I've investigated these stations scaled by a factor of 2.5, giving them diameters of 125m. These layouts are shown in Figures 19 through 25.

Table 1: LWDA1 Station Cable Lengths.

Station	Cable Length (m)
Grid 2m	3130
Spiral4	3456
Spiral1	3483
Spiral3	3504
Pats	3590
Spiral2	3607
Random 1.8m	4321
Random 2m	4347
Compact Fractal	5969
Exponential Fractal	6660

5.1. Metrics

Plots of the metrics for the LWA stations are given in this section. The same color/symbol key is used throughout the figures and is given below:

• = 1 arm spiral	□ = 2 arm spiral	○ = 3 arm spiral
⋆ = 4 arm spiral	• = Pat's	• = grid, 5m
• = random, 5m	• = compact fractal	□ = fractal

Beam Size

Beam Size is plotted in Figure 26. The fractal stations now have the largest beam sizes since they have smaller diameters and are centrally condensed.

Beam Efficiency

Plots of the beam efficiency metric are shown in Figure 27. Grating lobes appear on the horizon at 60 MHz for the grid, Pat's, and the spiral stations. These lobes keep the beam efficiency metric below 0.05 above 60 MHz and are due to the grid structure in each station. The fractal stations have the highest metrics above 60 MHz but also the lowest below ∼35 MHz.

Aperture Efficiency

Plots of the aperture efficiency metric are shown in Figure 28. The grating lobe problem above 60 MHz for stations with grid structures is a problem for the aperture efficiency metric too.

Cable Length

Table 2 gives cable lengths for these stations.

Table 2: LWA Station Cable Lengths.

Station	Cable Length
Compact Fractal	5969
Exponential Fractal	6660
Grid 5m	7824
Spiral4	8641
Spiral1	8703
Spiral3	8761
Pats	8975
Spiral2	9018
Random 5m	10867

5.2. The Grating Lobe Problem

For the Pat and spiral stations bad grating lobes appear above 60 MHz and devastate the beam and aperture efficiency metrics. These grating lobes are due to the central grid of the layouts. This section investigates how reducing the number of elements on the grid effects the magnitude of the lobes.

I generated a Pat station with a 4m grid and $d_{min} = 25$m, see Figure 29. This design has 120 elements on the central grid. I also created a station with a 4m grid but the radial stretching begins much closer to the center $d_{min} = 10.2$m, leaving only 24 elements on the grid. This is shown in Figure 30. Figures 31 and 32 show power pattern slices for these stations over frequency. It can be seen that the station with 24 elements on the grid has lower grating lobes, but still rather strong. I do not think this is an adequate solution to the problem.

There is another disadvantage to the reduced grid station. Physically, it is much larger, with a diameter of about 240m compared to 100m. The cable length needed for this station

is also much greater, 16360m compared to 7180m!

6. What's Next?

Grating lobes are a major problem for an LWA station. Any design with a grid structure spaced for low frequencies will produce bad grating lobes at higher frequencies. This wasn't a problem for LWDA1 stations since they were optimized for 74 MHz, at the high end of the frequency range. New station designs are needed for the LWA without central grids. The fractal stations did not develop grating lobes at high frequencies but their metrics were poor below 40 MHz. New designs need to be investigated, some possibilites are spiral designs where the spiral arms extend all the way to the center of the station. Replacing the central grid of Pat's design with a random arrangment is another possibility.

Future work on station configurations should include pointing the beam away from the zenith. Pointing the beam away from zenith will cause sidelobes that were below the horizon to appear opposite the direction of pointing. This may include grating lobes and would be very important.

An examination of the effects of tapering the grading function and the effects of amplitude and phase errors also need to be done.

More metrics quantifying the power pattern may be useful. Some metrics I proposed but haven't used so far include:

PowerRMS

The RMS of the power pattern over annuli centered on the beam direction. If the beam is pointed at the zenith then the annuli are rings of constant elevation. The PowerRMS metric should be calculated at several annuli close to and far from the main beam in order to sample inner and outer sidelobes

StdDev

The standard deviation of PowerRMS. A measure of the spread of power values from the RMS power. If the power pattern is fairly constant around the annulus the standard deviation will be low. If the annulus overlaps many sidelobes and nulls the standard deviation will be high.

SkewMetric

The skewness of the PowerRMS. The SkewMetric indicates the degree of asymmetry of the power pattern around an annulus.

REFERENCES

J. D. Bregman, G. H. Tan, W. Cazemier, and C. Craeye, "A wideband sparse fractal array for low frequency radio astronomy," *Proc. IEEE International Symposium on Antennas and Propagation*, Salt Lake City, July 2000.

J. D. Bregman, "Concept Design for a Low Frequency Array", *SPIE Conference on Radio Telescopes in Astronomical Telescopes and Instrumentation*, March 2000, Munich, SPIE Proc. 4015-3

J. D. Bregman, "Design concepts for a sky noise limited low frequency array", in *Proceedings NFRA SKA Symposium: Technologies for Large Antenna Arrays*, Dwingeloo, April 1999

This preprint was prepared with the AAS LaTeX macros v5.2.

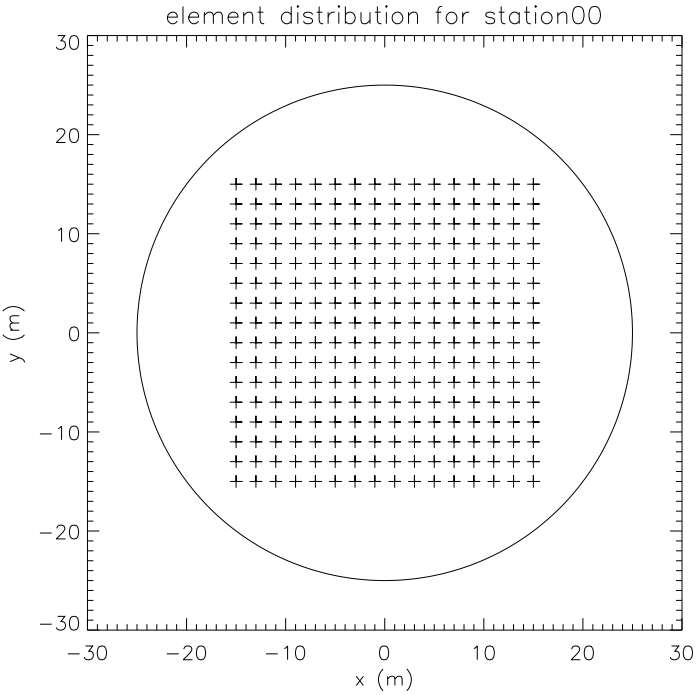

Fig. 1.— Grid design, 2m.

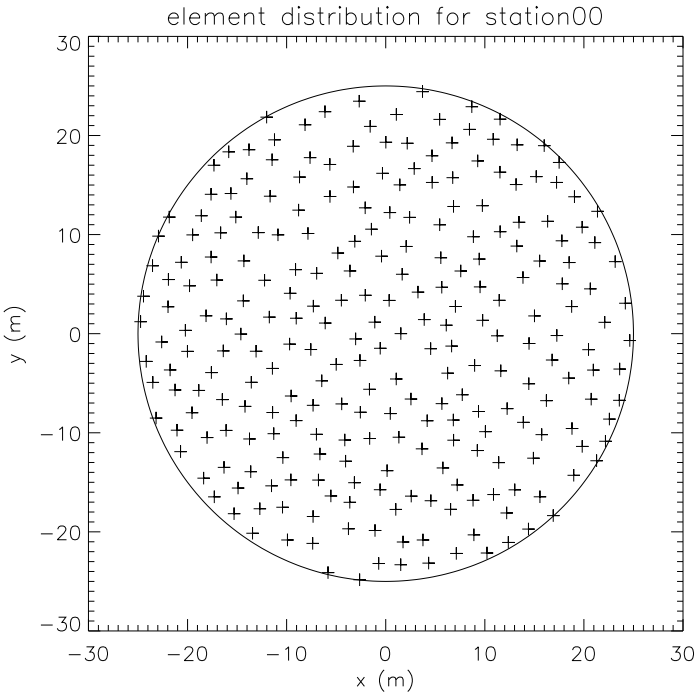

Fig. 2.— Random design, minimum separation = 2m.

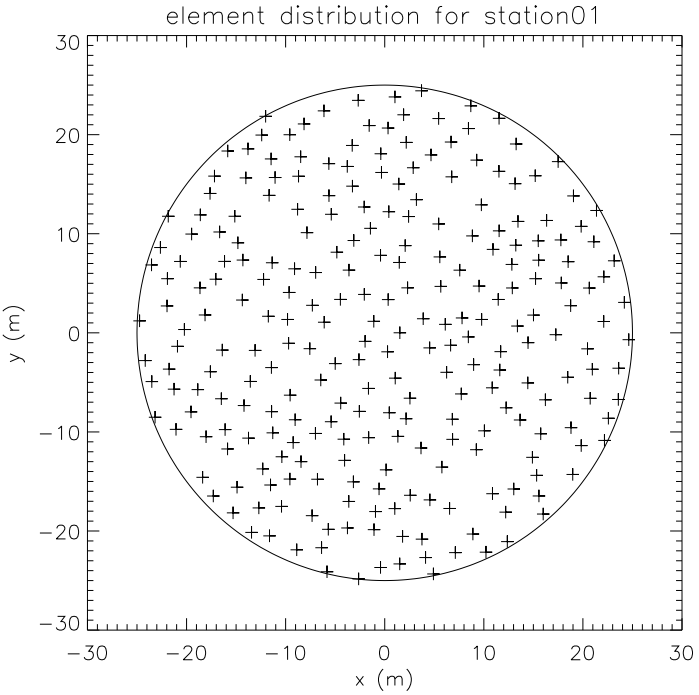

Fig. 3.— Another random design, minimum separation = 1.8m.

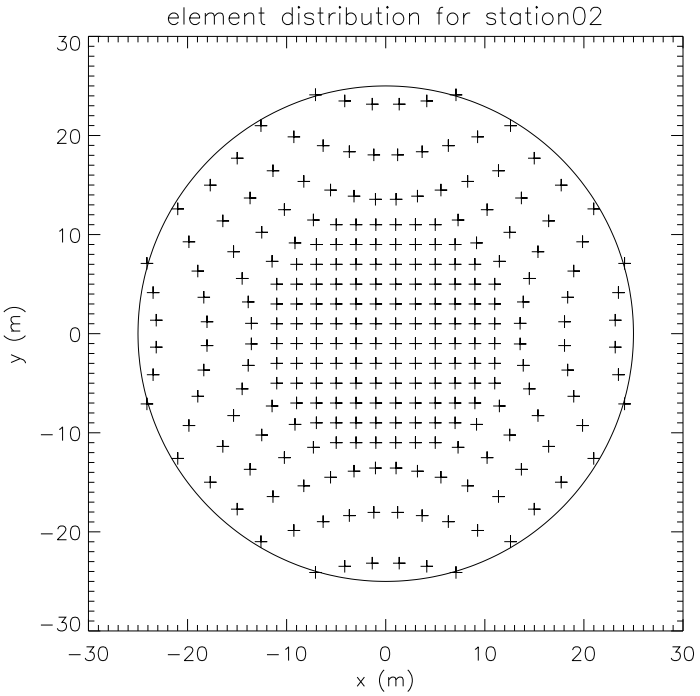

Fig. 4.— Pat's design.

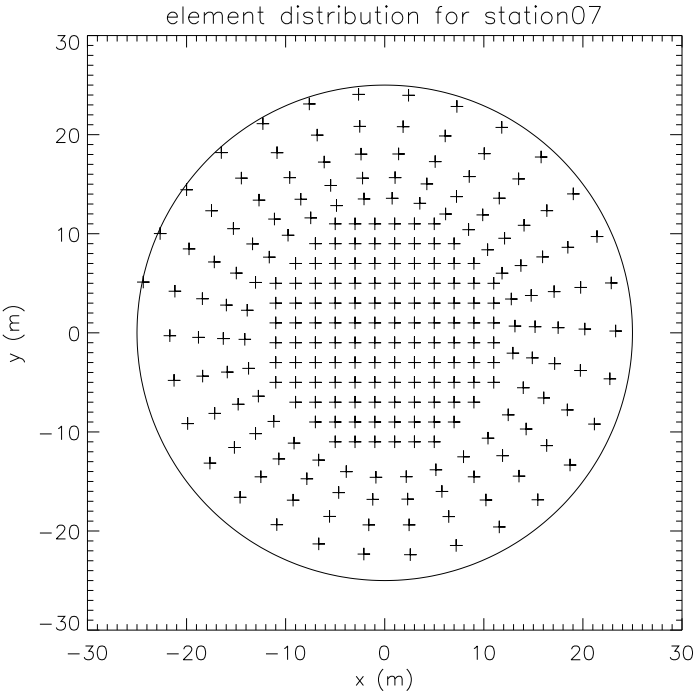

Fig. 5.— 1 arm spiral design.

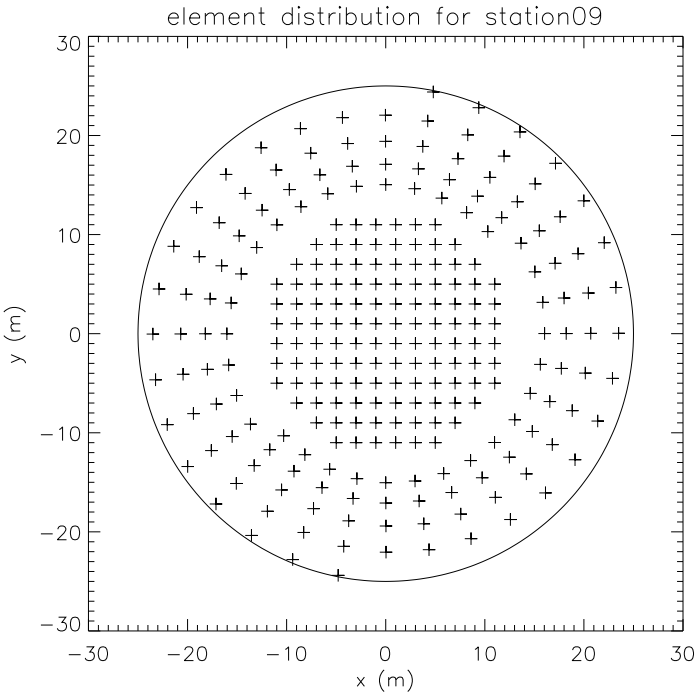

Fig. 6.— 2 arm spiral design.

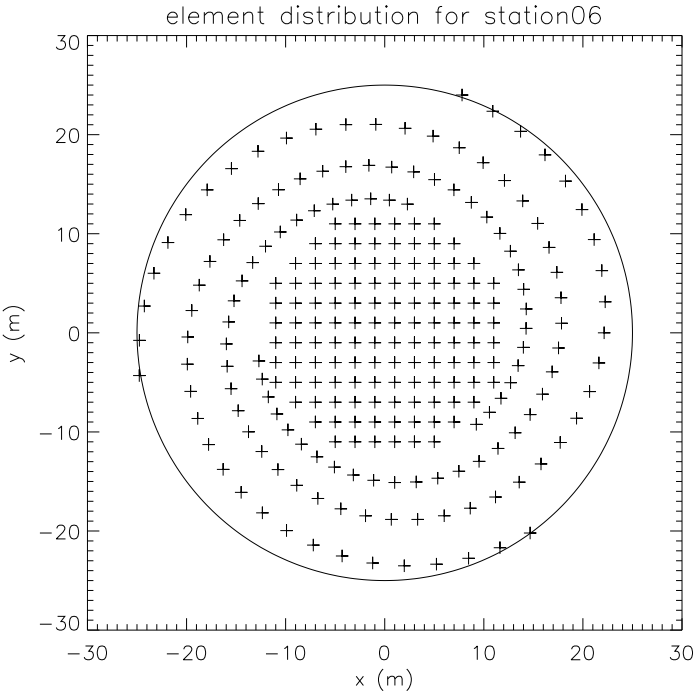

Fig. 7.— 3 arm spiral design.

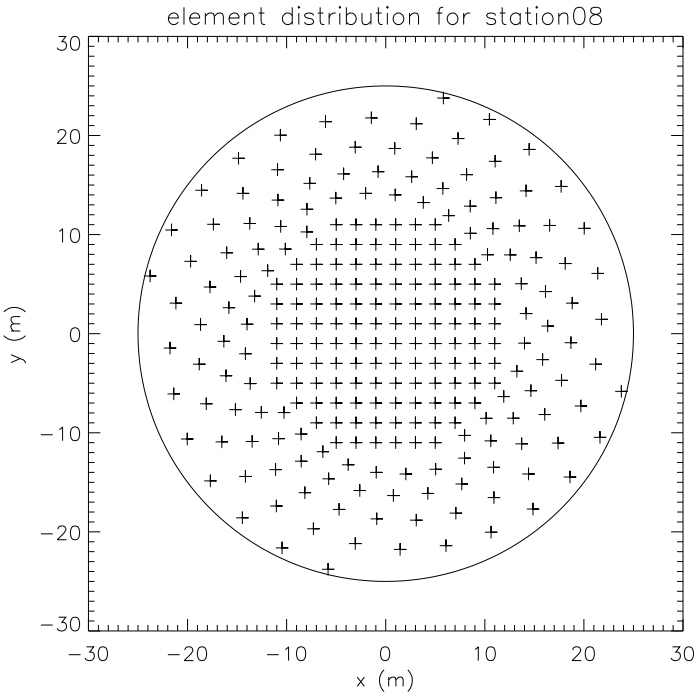

Fig. 8.— 4 arm spiral design.

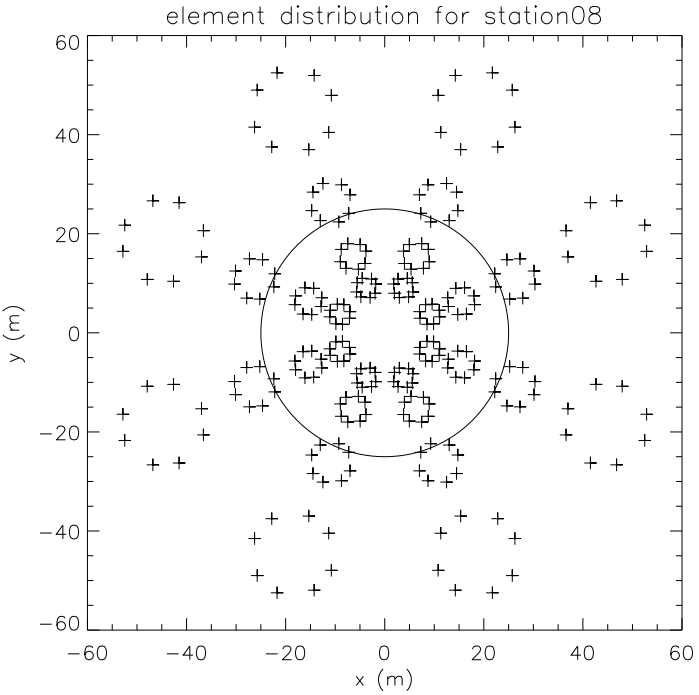

Fig. 9.— Fractal design, exponentially increasing ring radius.

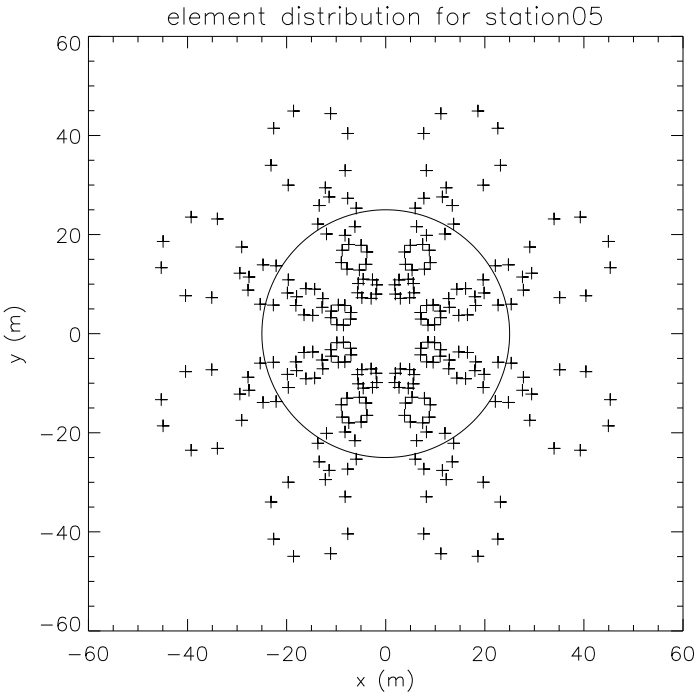

Fig. 10.— "Compact" fractal design.

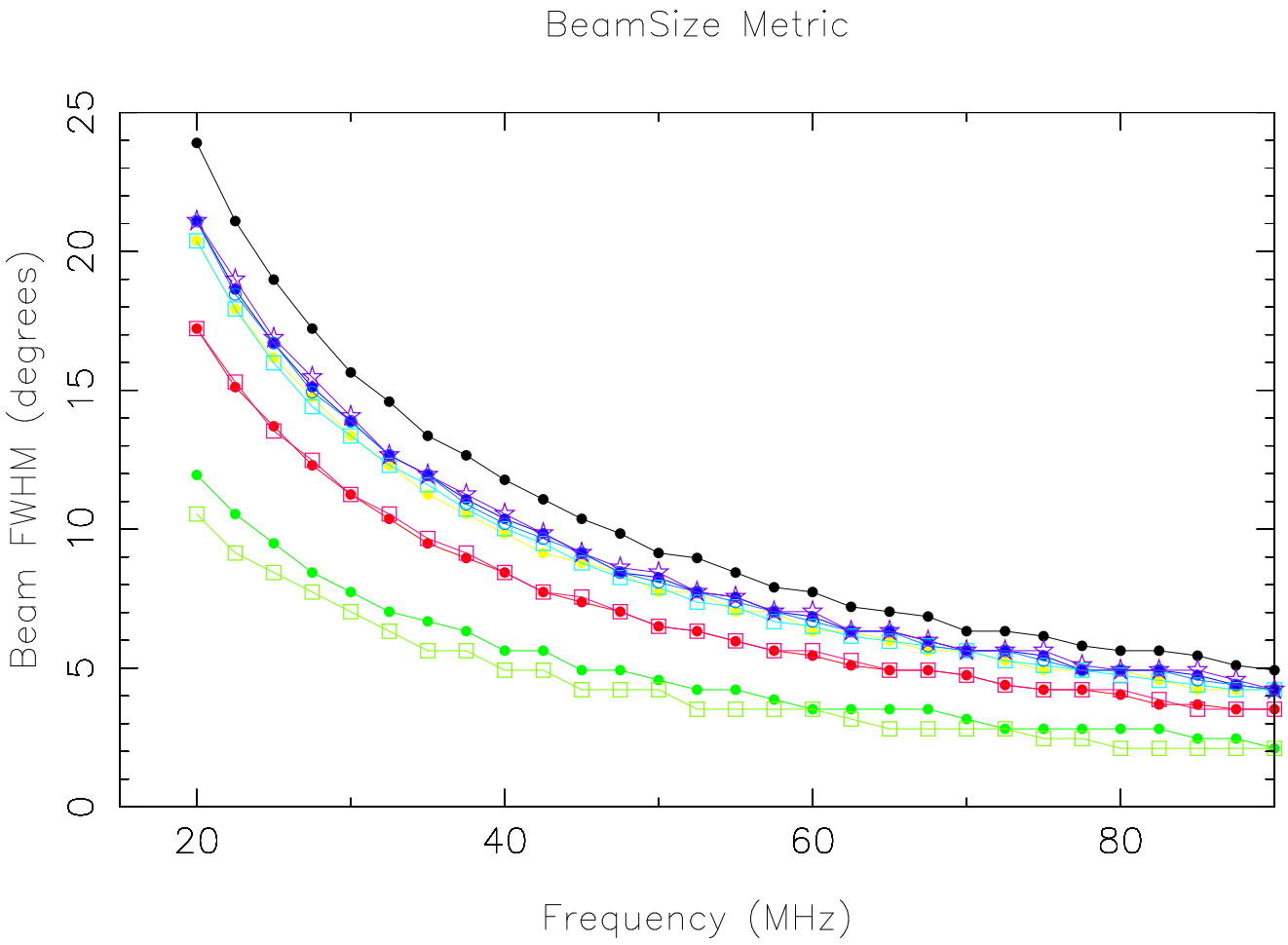

Fig. 11.— Beam sizes for LWDA1 configurations.

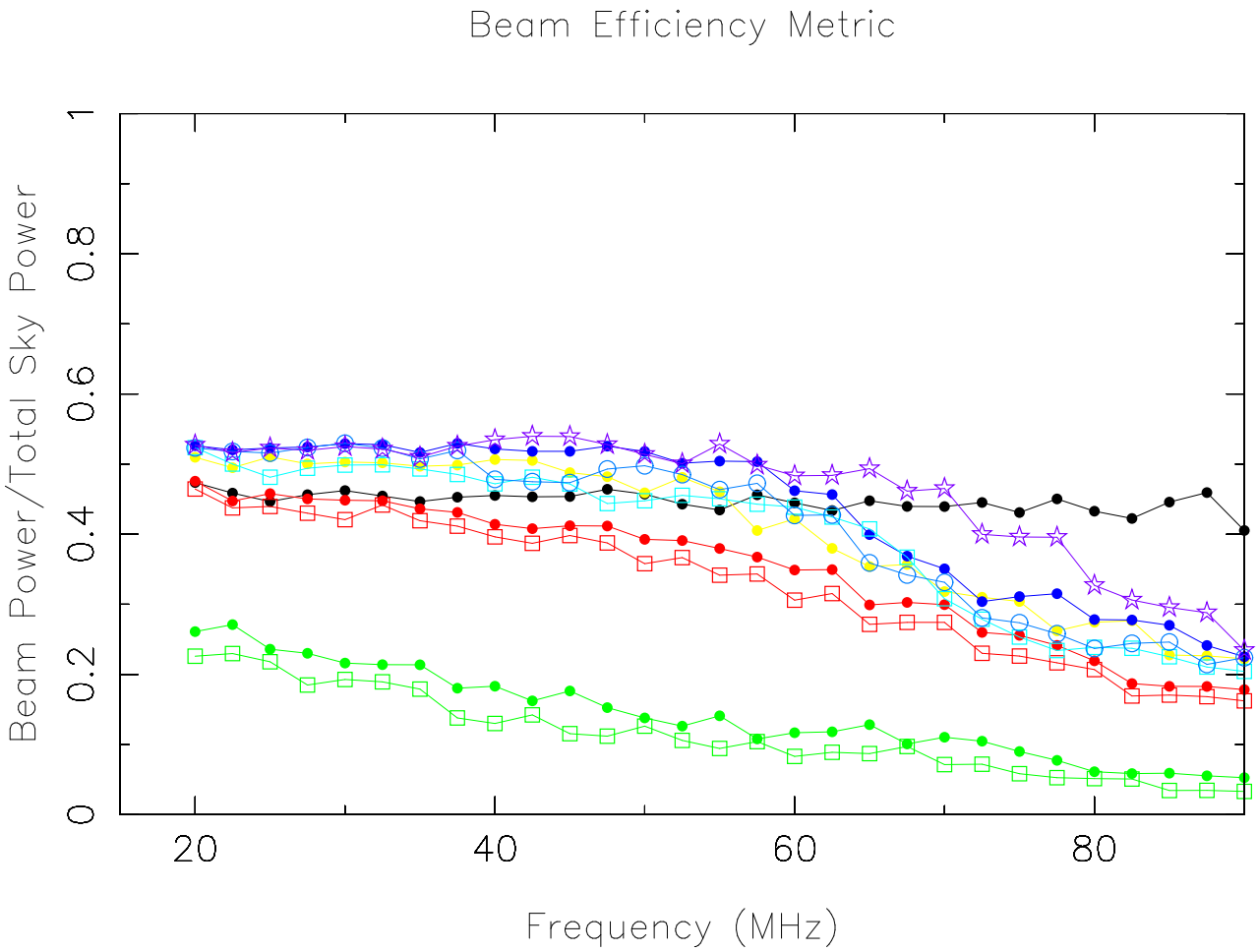

Fig. 12.— Beam efficiency for LWDA1 configurations.

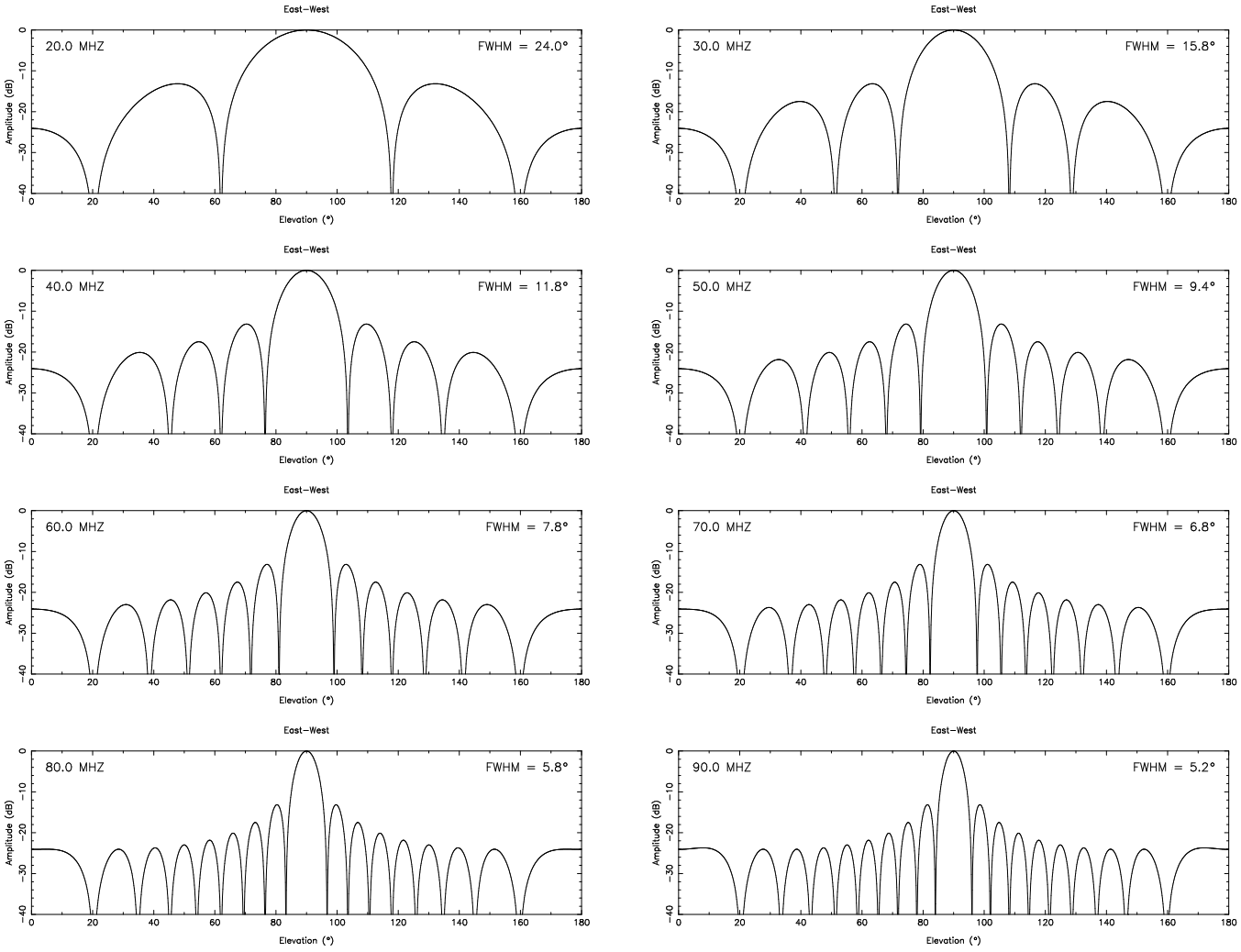

Fig. 13.— Slices through the 2m grid power pattern.

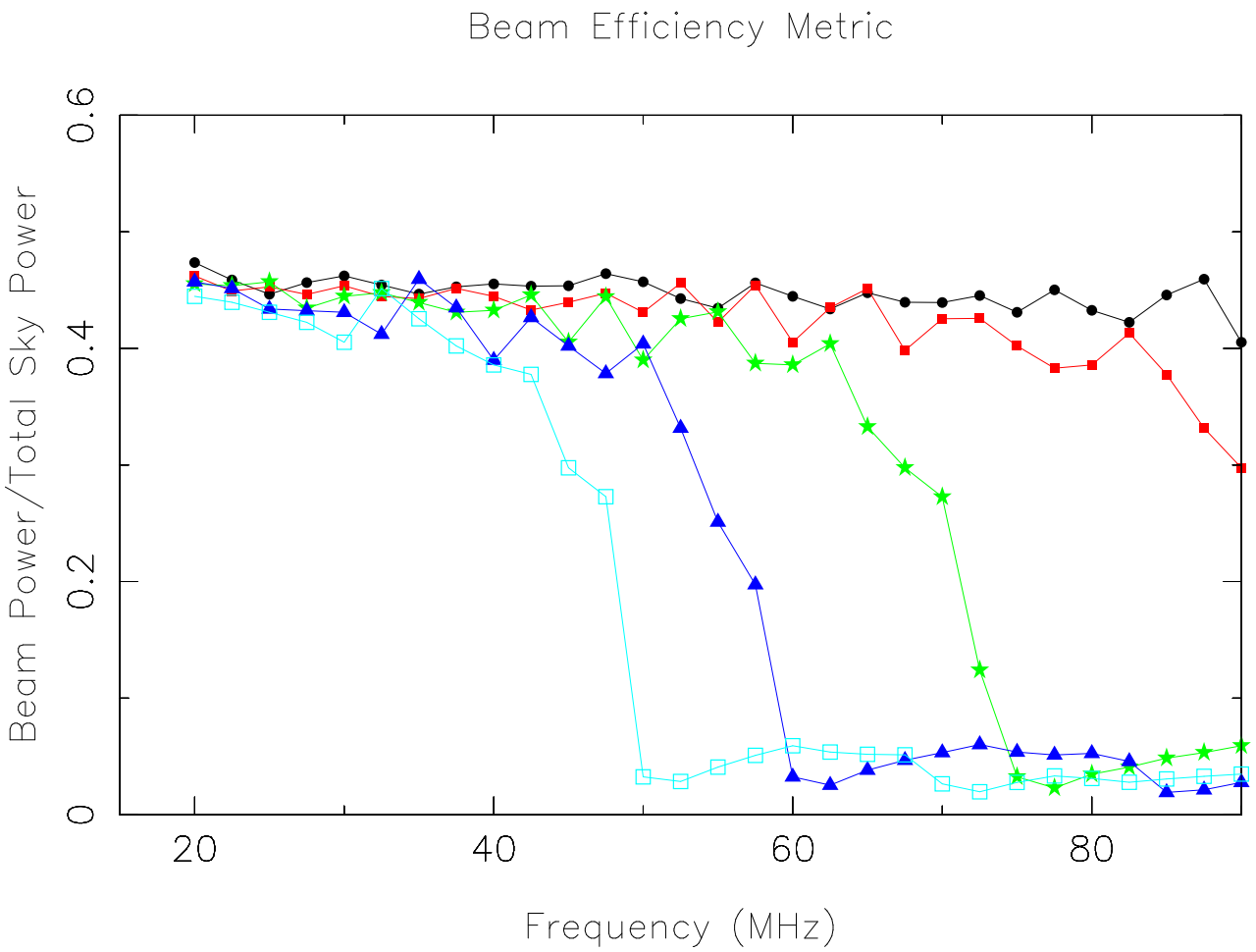

Fig. 14.— Beam efficiency for various size grid configurations. • = 2m, ■ = 3m, ★ = 4m, ▲ = 5m, □ = 6m

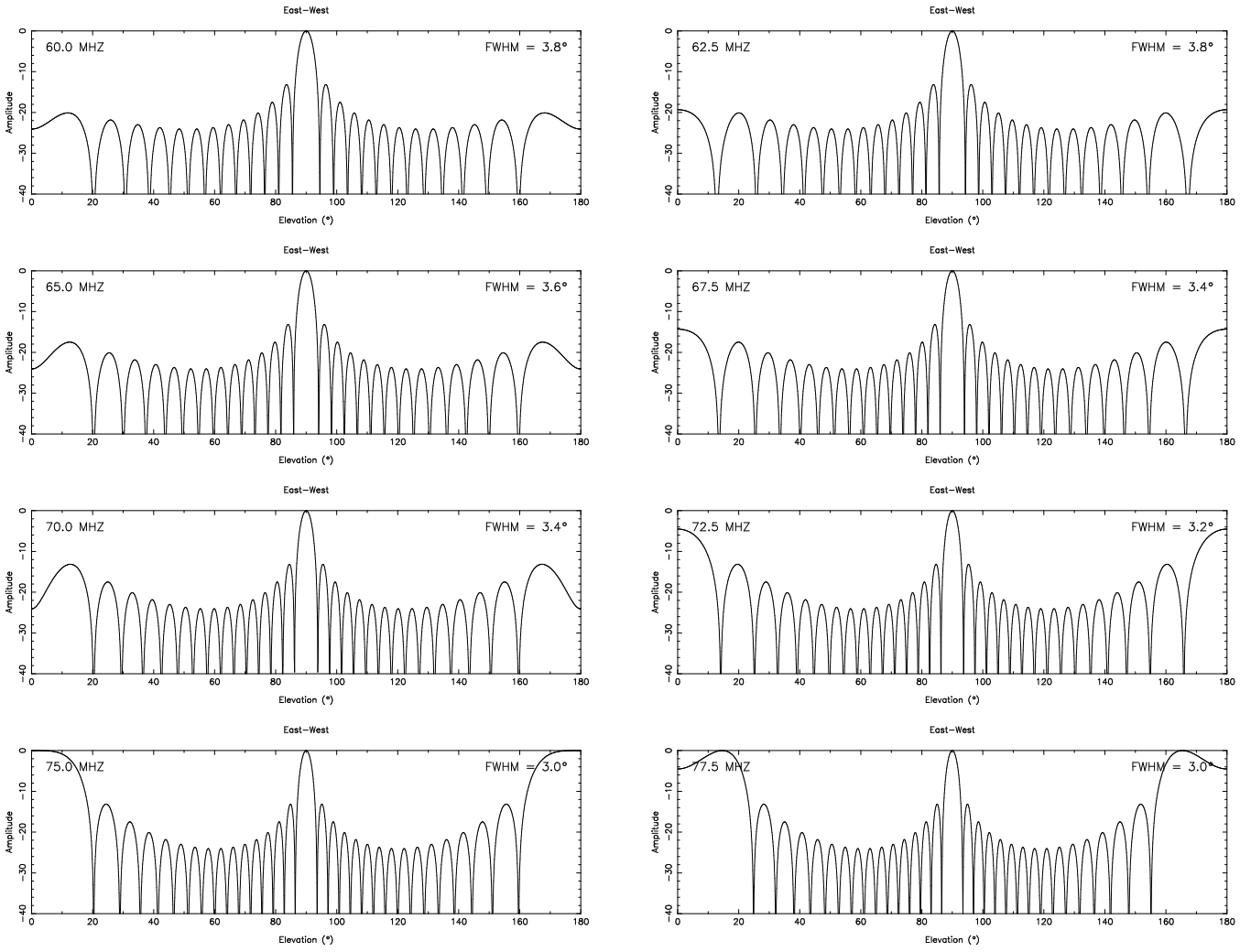

Fig. 15.— E-W slices of the power pattern for a 4m grid. Grating lobes appear on the horizon at 75 MHz.

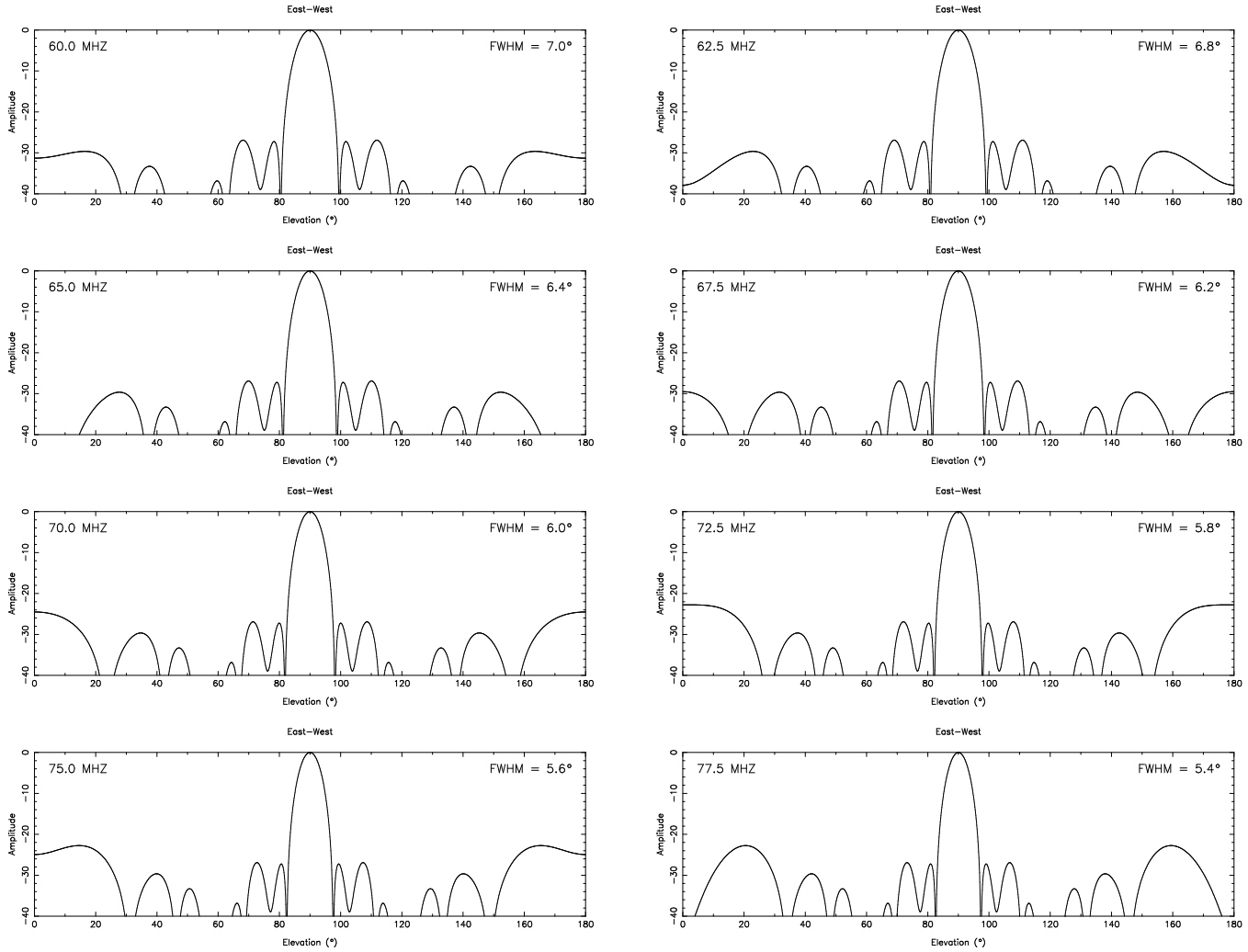

Fig. 16.— E-W slices of the power pattern for the 4 armed spiral.

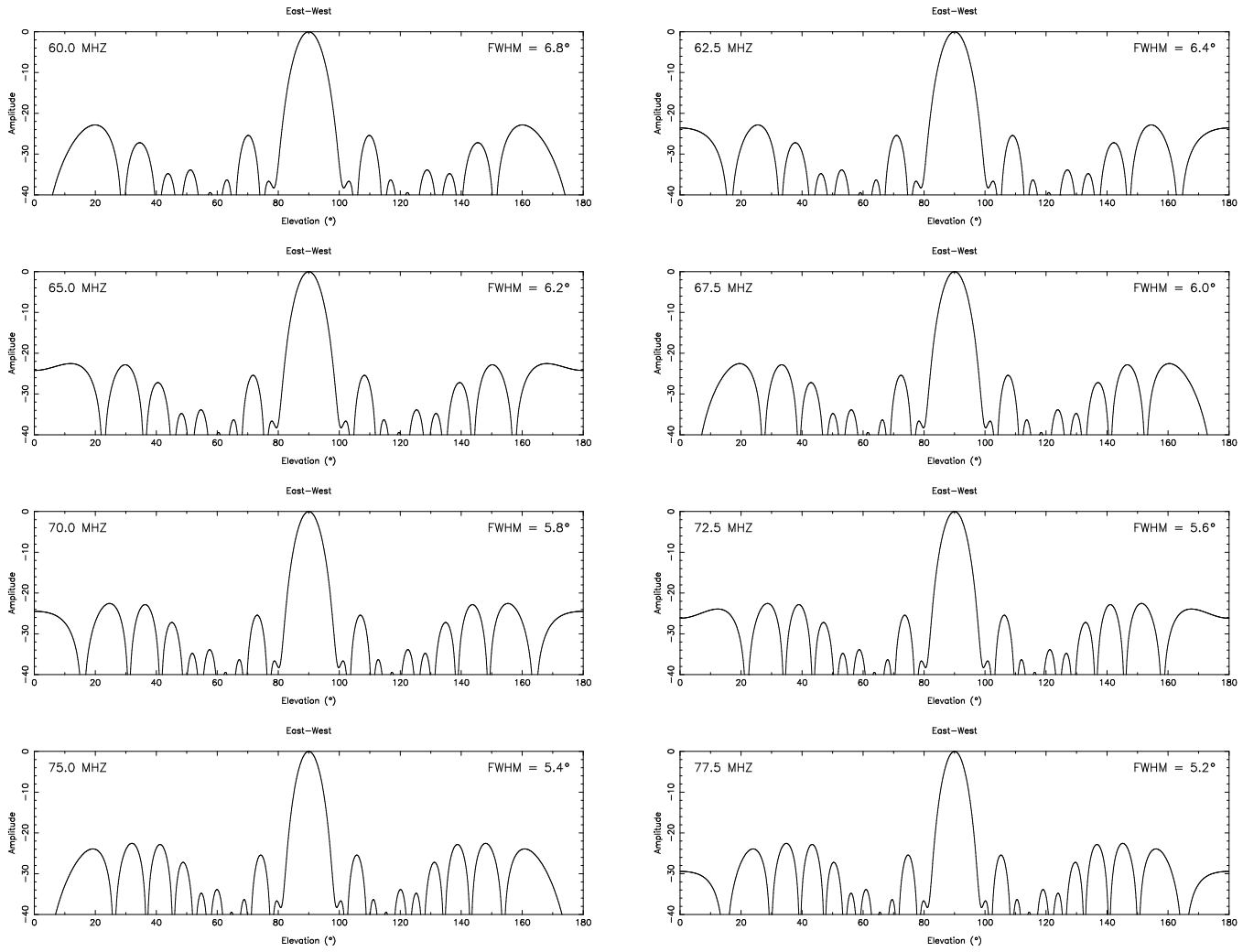

Fig. 17.— E-W slices of the power pattern for Pat's station.

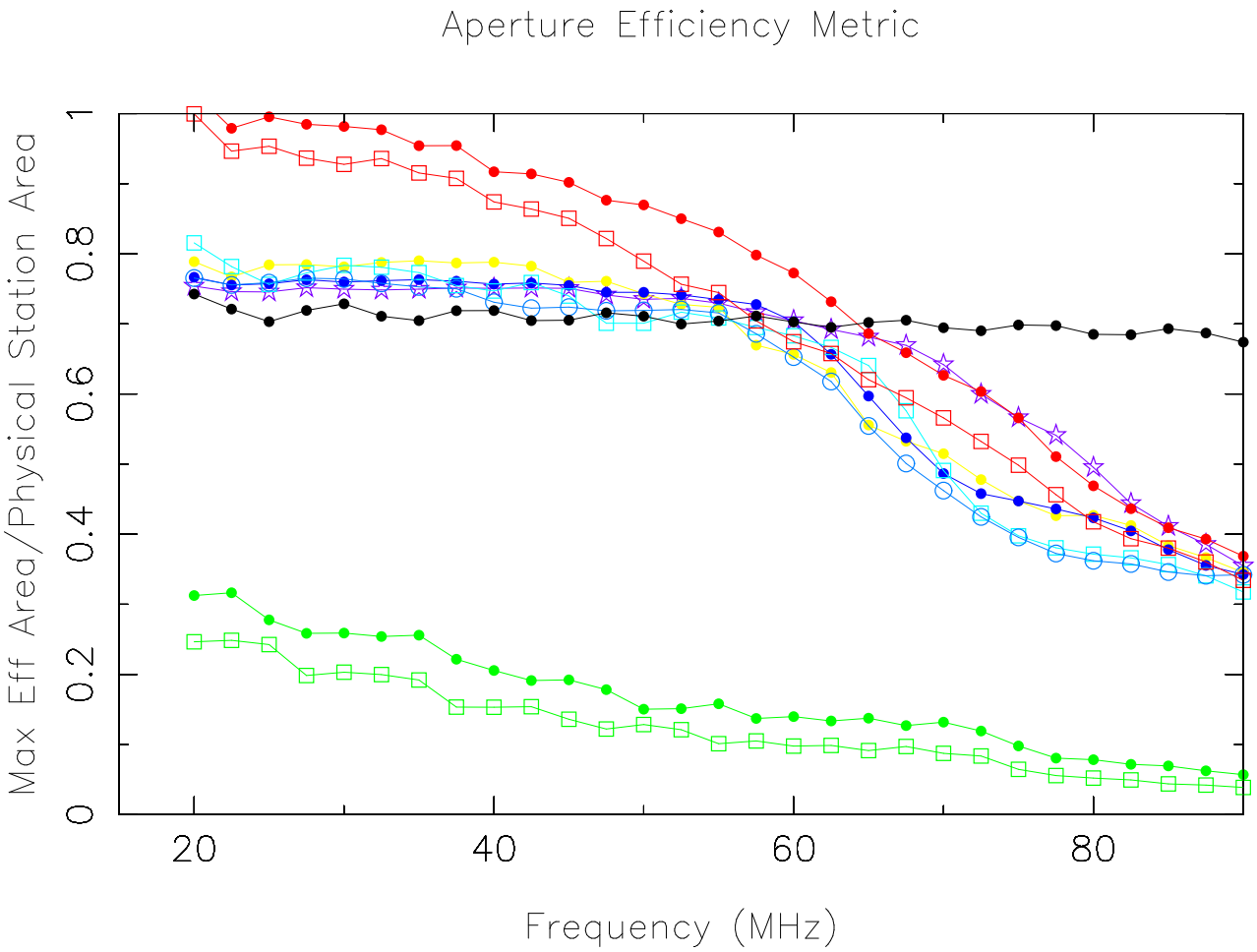

Fig. 18.— Aperture efficiency for LWDA1 configurations.

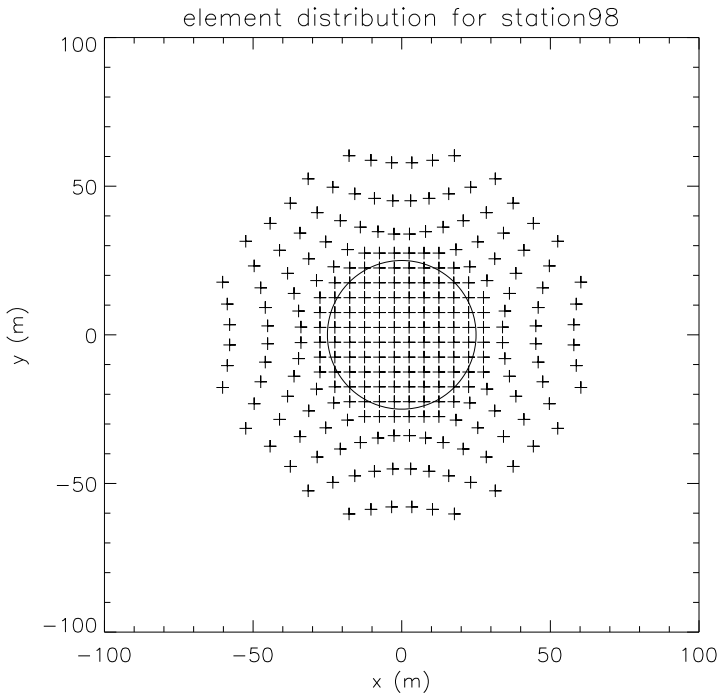

Fig. 19.— Pat's design scaled by a factor of 2.5

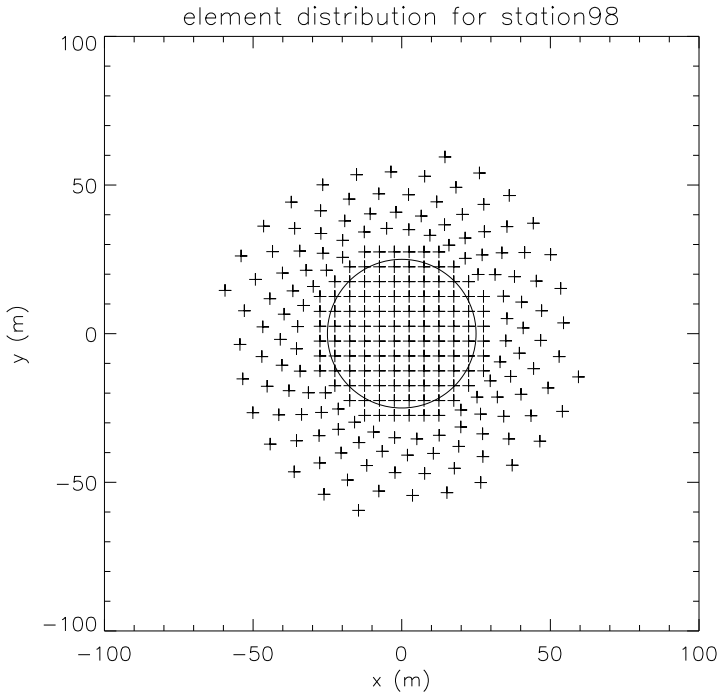

Fig. 20.— 4 arm spiral design scaled by a factor of 2.5

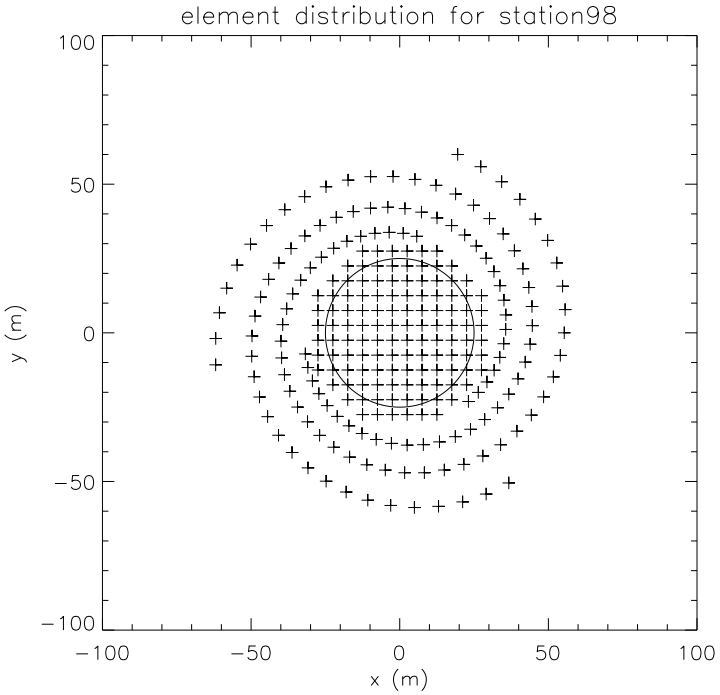

Fig. 21.— 3 arm spiral design scaled by a factor of 2.5

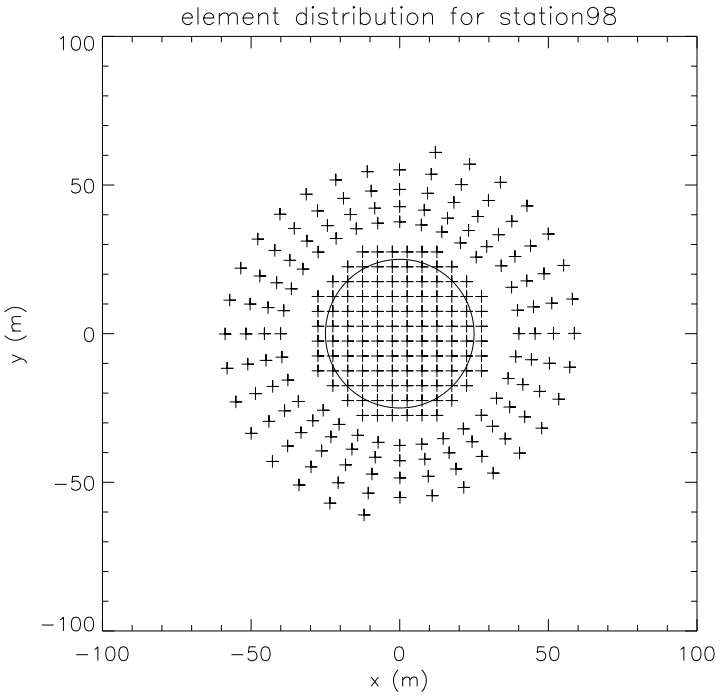

Fig. 22.— 2 arm spiral design scaled by a factor of 2.5

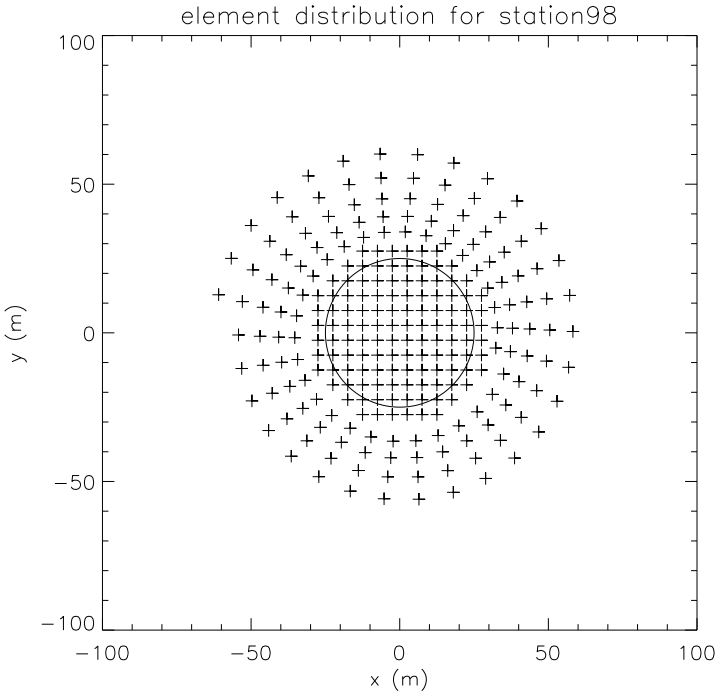

Fig. 23.— 1 arm spiral design scaled by a factor of 2.5

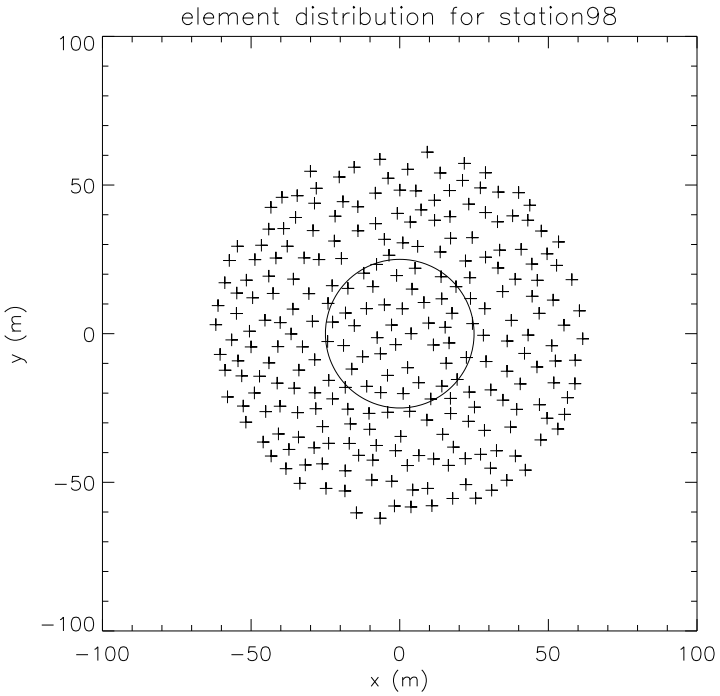

Fig. 24.— Scaled random design, minimum separation = 5m.

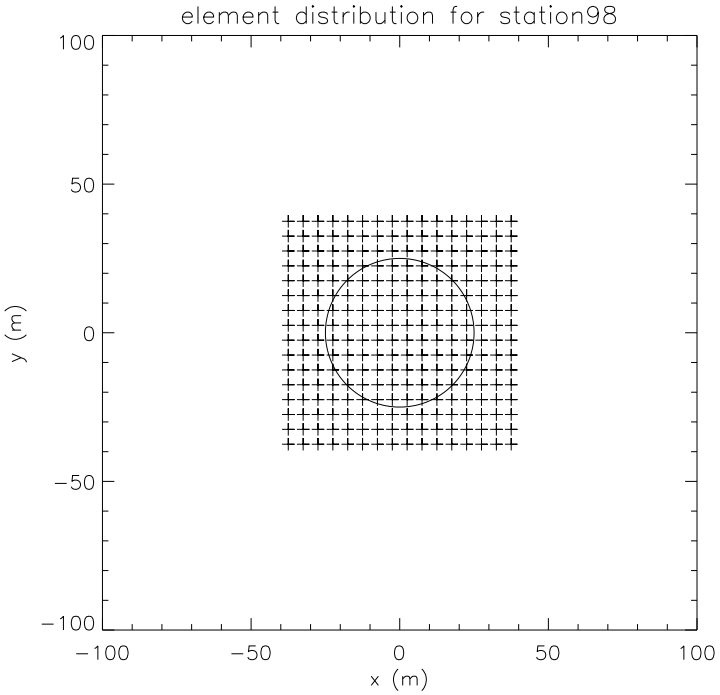

Fig. 25.— Grid, element spacing = 5m.

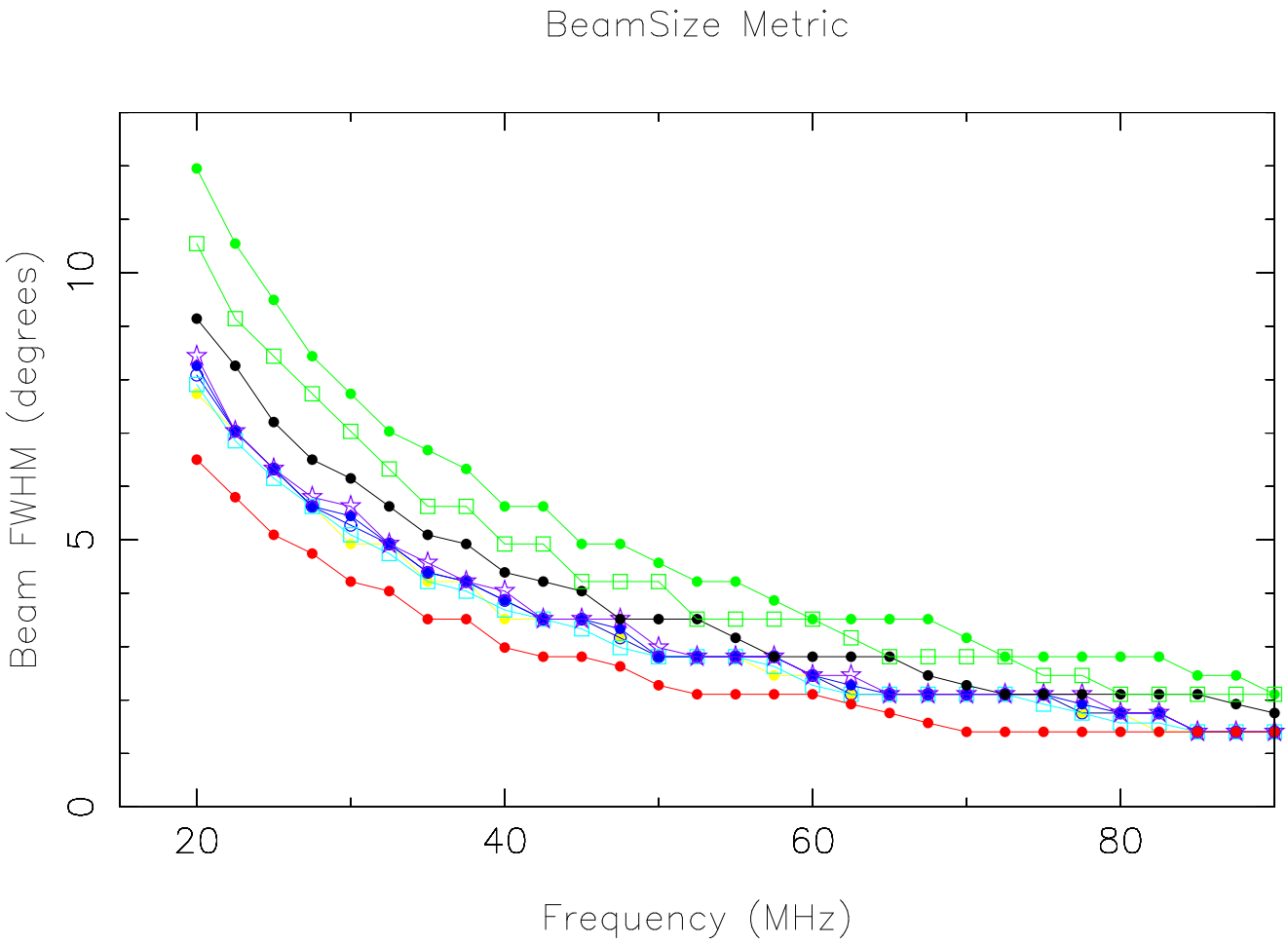

Fig. 26.— Beam size for LWA stations.

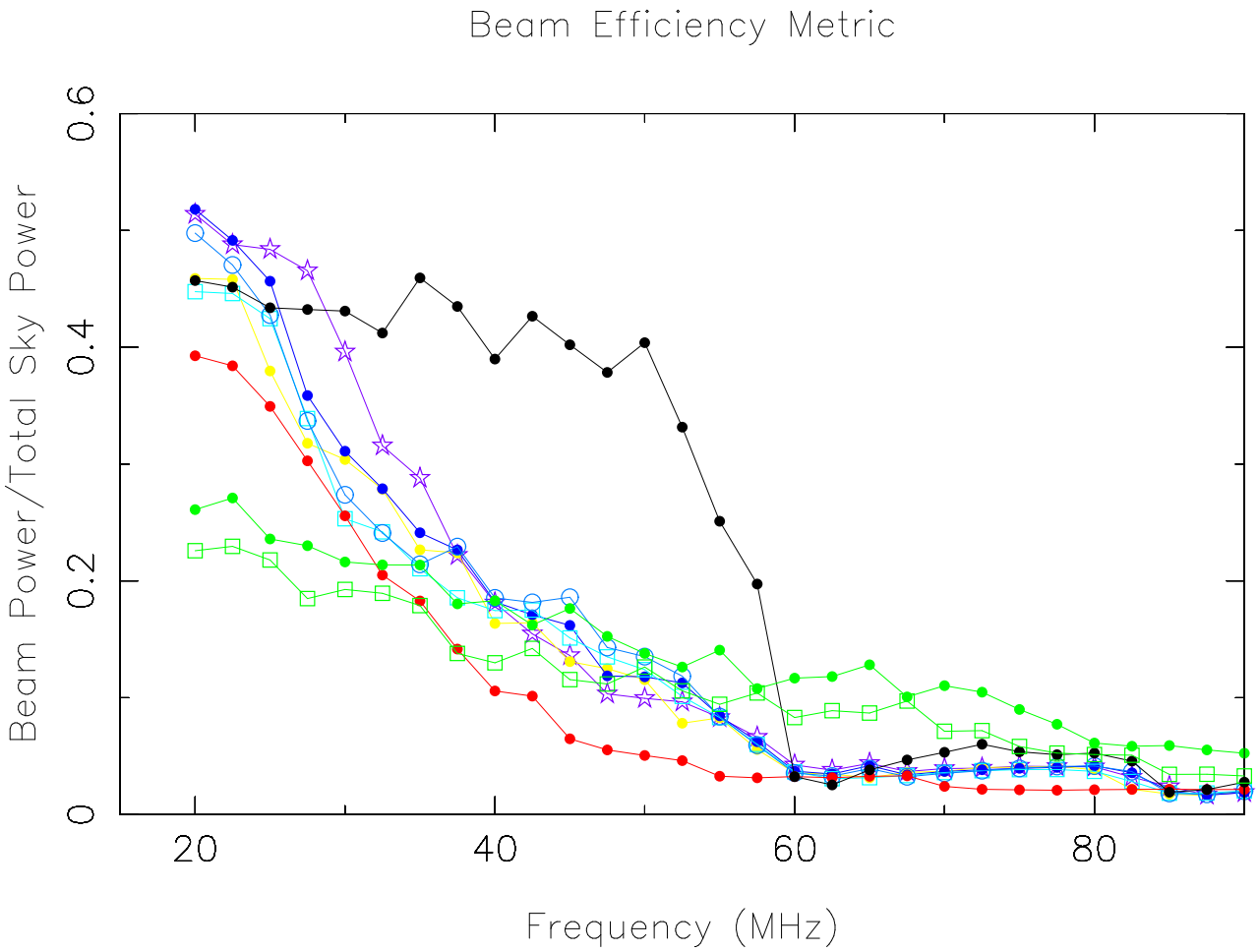

Fig. 27.— Beam efficiency for LWA stations.

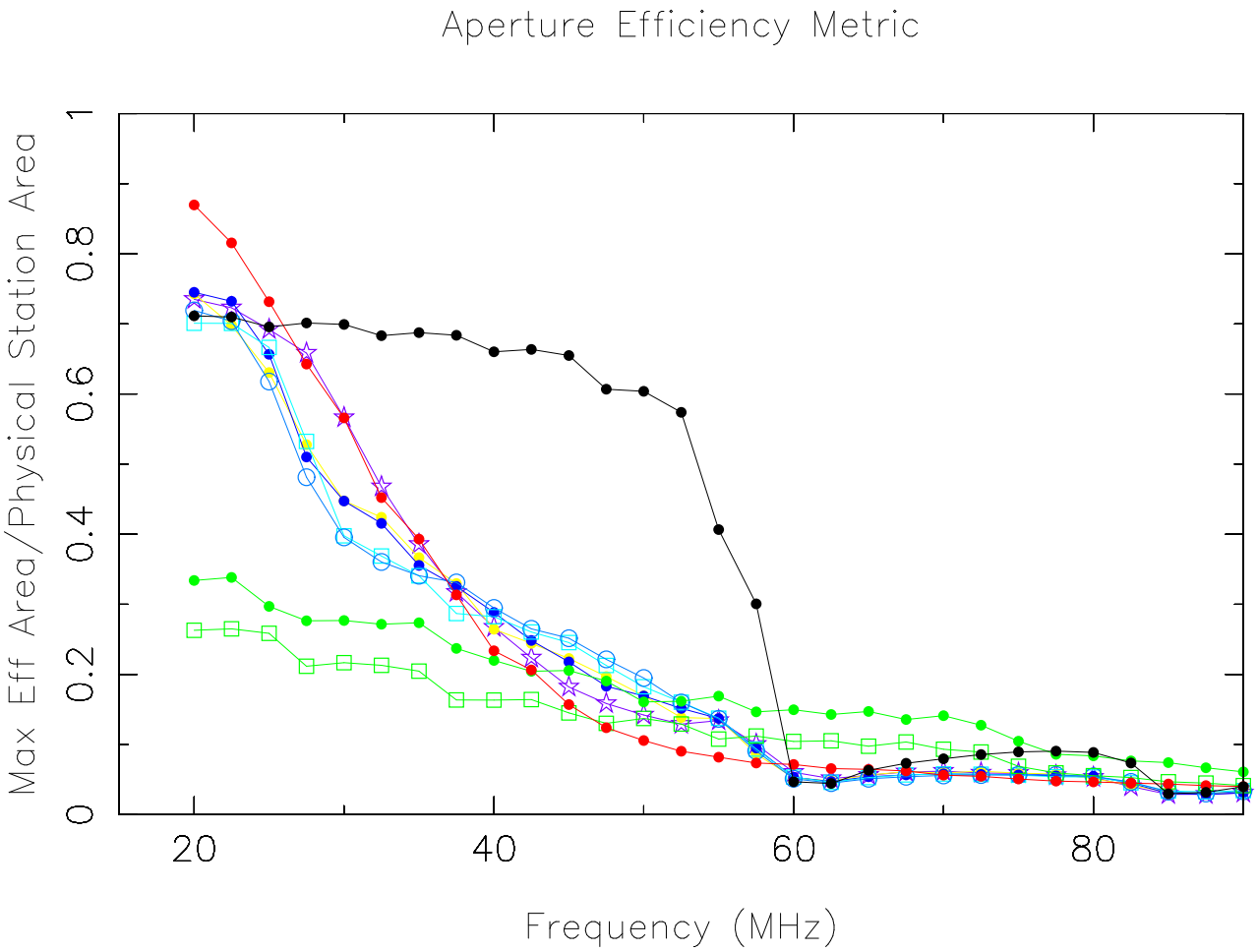

Fig. 28.— Aperture efficiency for LWA stations.

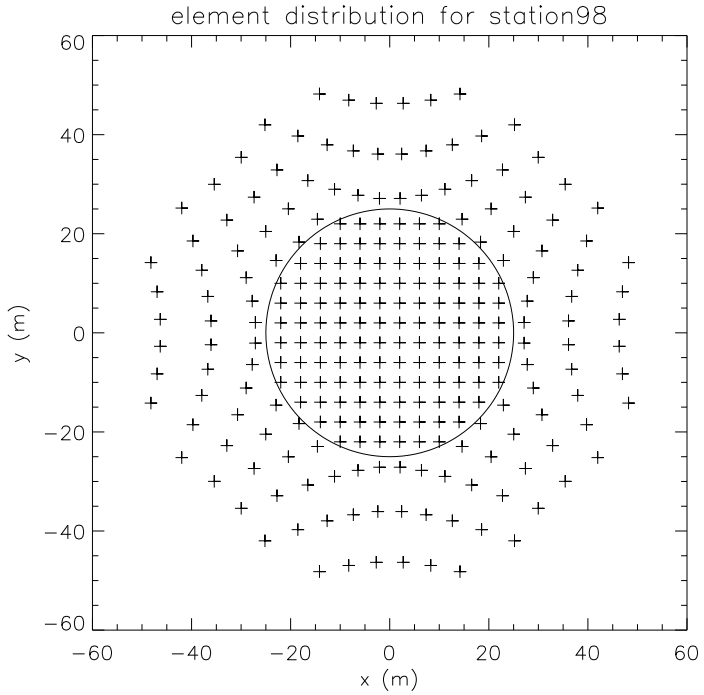

Fig. 29.— Pat's design with 120 elements on a 4m grid.

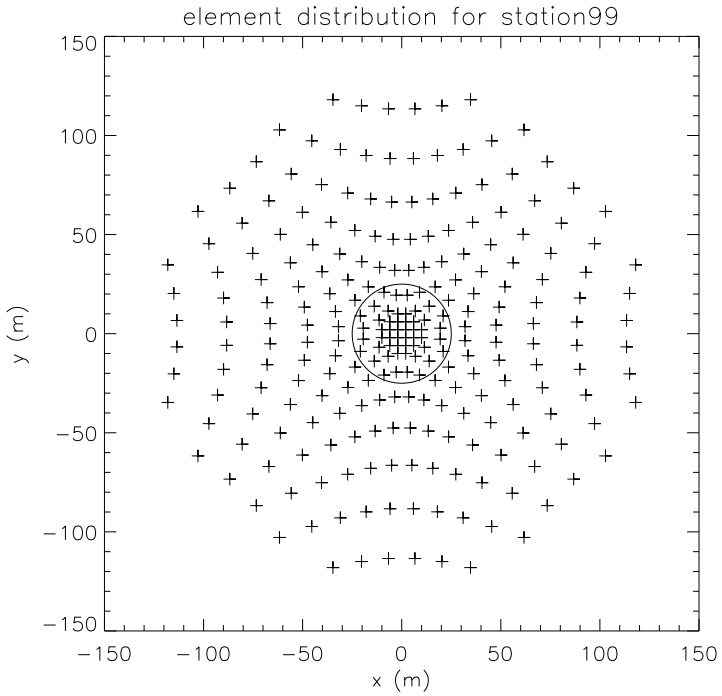

Fig. 30.— Pat's design with 24 elements on a 4m grid.

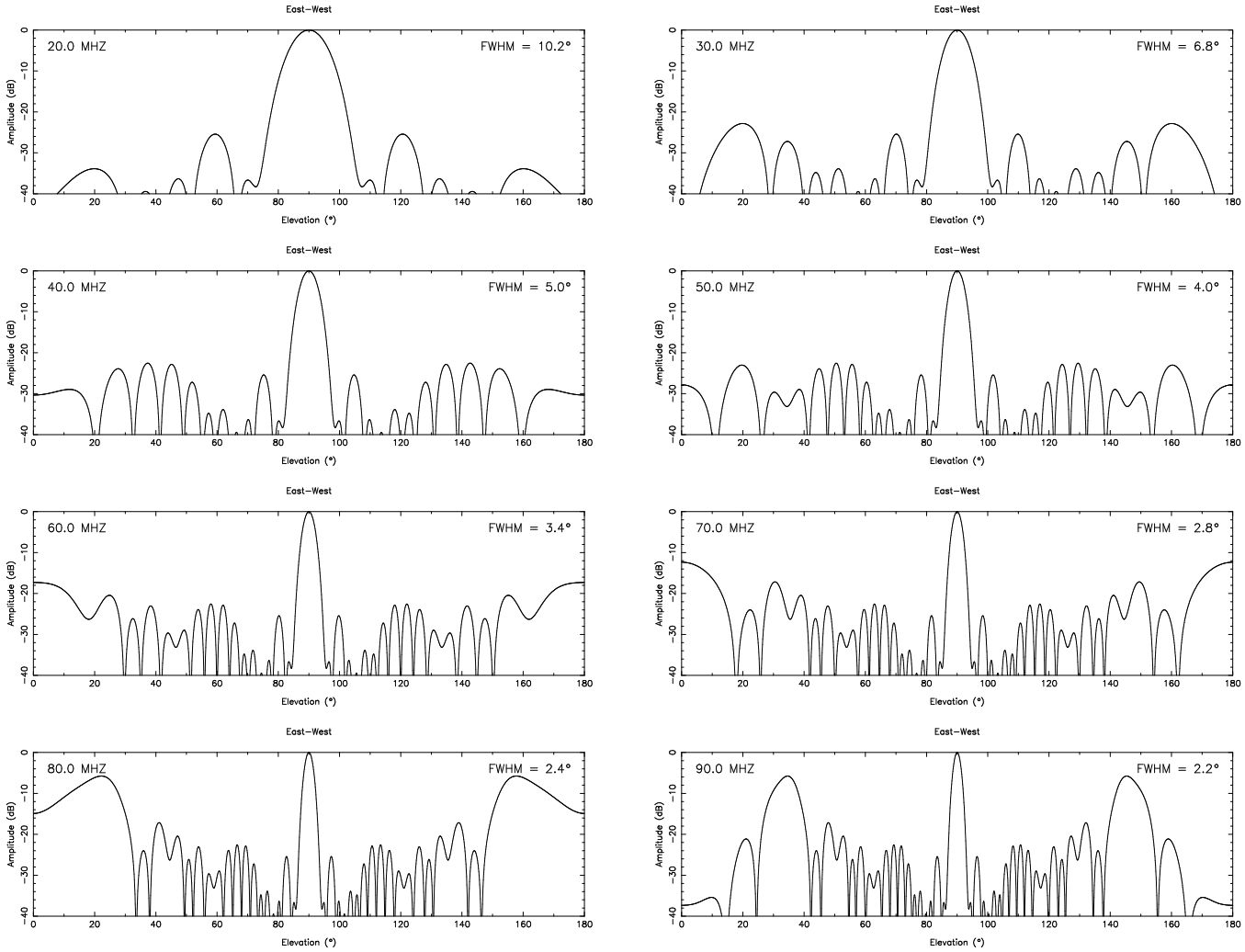

Fig. 31.— E-W power slices for Pat's station with 120 elements on grid.

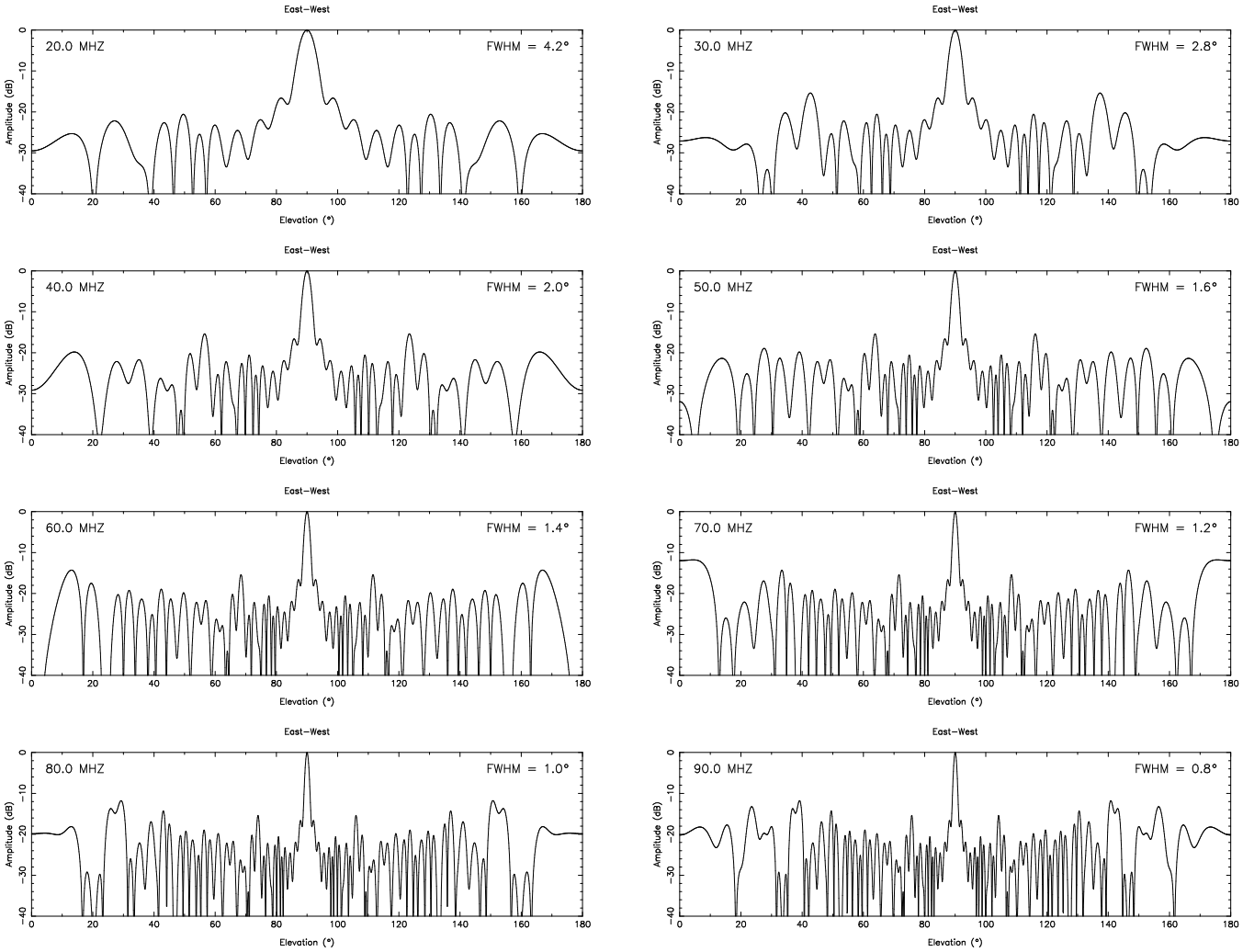

Fig. 32.— E-W power slices for a Pat station with 24 elements on grid.